International Journal of Refrigeration 120 (2020) 90–96

Contents lists available at ScienceDirect

International Journal of Refrigeration

journal homepage: www.elsevier.com/locate/ijrefrig

Traveling-wave thermoacoustic refrigerator for room temperature application

Xin Wang[a,b], Zhanghua Wu[a,*], Limin Zhang[a], Jianying Hu[a], Ercang Luo[a,*]

[a] Key Laboratory of Cryogenics, Chinese Academy of Sciences, Beijing 100190, China
[b] University of Chinese Academy of Sciences, Beijing 100049, China

ARTICLE INFO

Article history:
Received 17 April 2020
Revised 19 August 2020
Accepted 24 August 2020
Available online 27 August 2020

Keywords:
Traveling-wave thermoacoustic refrigerator
Room temperature refrigeration
Multi-stage refrigerator

ABSTRACT

As a new type of refrigeration technology, the traveling-wave thermoacoustic refrigerator offers advantages that include high efficiency, reliability and environmental friendliness. To date, because of problems such as low power utilization and high power recovery losses, traveling-wave thermoacoustic refrigerators for use in room temperature applications have not been widely studied. In this paper, following an investigation of the traditional single-stage traveling-wave thermoacoustic refrigerator, a multi-stage traveling-wave thermoacoustic refrigerator is proposed and the working mechanism of this refrigerator is studied numerically using SAGE software. The calculation results show that the proposed multi-stage traveling-wave thermoacoustic refrigerator can enhance the utilization of the input acoustic work effectively, thereby improving the cooling power of the refrigerator with high cooling efficiency. As a result, the cooling power increases from 2.17 kW for a single-stage refrigerator to 6.42 kW for a seven-stage refrigerator, while the acoustic work utilization rate increases from 0.26 to 0.82, and the coefficient of performance changes from 2.60 to 3.19. The calculation results also indicate that three to five stages may be most suitable for the multi-stage traveling-wave thermoacoustic refrigerator when working within the temperature range of interest here by striking a balance between cooling efficiency and cooling power.

Réfrigérateur thermoacoustique à ondes progressives pour une application à température ambiante

Mots clés: Réfrigérateur thermoacoustique à ondes progressives; Froid à température ambiante; Réfrigérateur multiétagé

1. Introduction

Refrigeration technologies play a number of important roles in daily life. Some of these refrigerators, such as air conditioners and domestic refrigerators, operate within the room temperature range. To date, several technologies have been applied to room temperature refrigeration, including vapor compression refrigeration technology, absorption refrigeration technology, adsorption refrigeration technology and magnetic refrigeration technology. Vapor compression-type refrigerators are the most widely used refrigerators worldwide and offer the advantage of high efficiency, but they also usually have associated environmental problems caused by the working substances used (Jatinder and Jagdev, 2017). Absorption and adsorption chillers are driven by low-grade thermal energy and are thus most suitable for low-temperature waste heat or solar thermal applications. However, the efficiency and the power density of these chillers are low (Athanasios and Alexio-Spyridon, 2019; Ahmed, 2017). In addition, the working substances of the absorption chillers are generally corrosive to metals (Andrea et al., 2015). Magnetic refrigeration is a new green refrigeration technology with remarkable energy saving effects; however, the operating temperature range of this type of refrigerator is not very large and the technology is still under development (Behzad and Bjorn, 2018).

The thermoacoustic refrigerator is a new type of refrigerator that is capable of producing cooling capacities ranging from

* Corresponding authors.
E-mail addresses: zhhwoo@mail.ipc.ac.cn (Z. Wu), ecluo@mail.ipc.ac.cn (E. Luo).

https://doi.org/10.1016/j.ijrefrig.2020.08.021
0140-7007/

Nomenclature

COP	coefficient of performance
SWTAR	standing wave thermoacoustic refrigerator
TWTAR	traveling wave thermoacoustic refrigerator
RTHX	room temperature heat exchanger
REG	regenerator
CHX	cold heat exchanger
TBT	thermal buffer tube
Symbols	
p	pressure fluctuation (Pa)
U	volume velocity (m^3/s)
θ_{pU}	phase difference between p and U (deg)
Q_c	cooling power (kW)
W_a	acoustic work (kW)
W_{in}	inlet acoustic work (kW)
W_{out}	outlet acoustic work (kW)
η	utilization rate of acoustic work

room temperature down to the liquid hydrogen temperature (Mckelvey, 1995; Radebaugh et al., 1990; Hu et al., 2007). Based on the thermoacoustic effect, the thermoacoustic refrigerator can pump heat from low temperatures to the ambient temperature by consuming acoustic work. Thermoacoustic refrigerators offer several outstanding advantages. First, they are environmentally friendly because they use inert gases such as helium and nitrogen as their working substances. Second, thermoacoustic refrigerators offer great flexibility in terms of their drive methods. These devices can not only be powered by electric linear compressors but also can be powered by heat-driven thermoacoustic heat engines. Finally, the thermoacoustic refrigerator itself usually contains no moving parts, which will lead to high reliability.

Depending on the different acoustic field conditions used in the regenerator, thermoacoustic refrigerators can be divided into standing-wave and traveling-wave types. The standing-wave thermoacoustic refrigerator (SWTAR) has low thermal efficiency because of the irreversible thermodynamic process that occurs between the working gas and the solid wall in the regenerator. In contrast, the traveling-wave thermoacoustic refrigerator (TWTAR) can realize higher efficiency because of its use of a reversible thermodynamic cycle. Additionally, recovery of the outlet acoustic work, which can then be fed back to the input, is another method that helps to ensure the high efficiency of the TWTAR, particularly in room temperature cooling applications. Ceperley (1979) proposed the concept of the traveling-wave thermoacoustic engine. This work also indicated the way toward development of the TWTAR. At present, the TWTAR for operation at room temperature range has two main configurations. The first is the single-unit loop configuration-type TWTAR. In this system, the refrigerator has only one refrigerator core and the outlet is connected to its inlet using a phase shifter. The phase shifter can be composed of well-designed tubes or mass-spring units and is used to vary the pressure and volume velocity phase angles based on its acoustic inertance and capacitance characteristics. Additionally, the outlet acoustic work of the refrigerator is fed back to the inlet as part of the input acoustic work. Swift et al. (1999) invented this type of TWTAR and greatly improved the cooling efficiency. Poese (2004) designed an electrically-driven TWTAR that produced a cooling power of 120 W at 248.9 K. This TWTAR was later used by the Ben & Jerry's company to preserve their ice cream. Luo et al. (2006) developed a heat-driven TWTAR that produced a cooling power of 250 W at 251.4 K. Bassem et al. (2011) designed an electrically-driven TWTAR that produced 11 W of cooling power at 270 K. In the same year, Yu et al. (2011) designed another heat-driven TWTAR and obtained cooling powers of 340 W and 469 W at the cooling temperatures of 253 K and 273 K respectively. The final system is the multi-unit loop configuration-type TWTAR. In this system, several engine cores and refrigerator cores are connected end-to-end using slim resonant tubes. Similar to the single-unit TWTAR, these tubes can not only be used to adjust the phase angles of the pressure and velocity waves but also can transfer the outlet acoustic work from one unit to the next unit. Blok (2012) developed a system of this type that had one refrigerator core driven by three engine cores. This system produced 95 W of cooling power at 228 K. Wang et al. (2019) designed a similar heat-driven TWTAR that used three engine cores and three refrigerator cores. In their experiments, a total cooling power of 4.5 kW was produced at 283 K. Xu et al. (2020) provided a theoretical analysis of a proposed looped, thermoacoustically-driven refrigerator for low-grade heat utilization. The results show that proposed system can achieve 2.7 kW of cooling power at 270 K.

2. System Model

As shown in Fig. 1, the multi-stage TWTAR is composed of multiple thermoacoustic refrigerator cores. Each core consists of three parts, which are a room temperature heat exchanger (RTHX), a regenerator (REG) and a cold heat exchanger (CHX). These components are serially connected from the inlet to the outlet within each core. Adjacent cores are connected using thermal buffer tubes (TBTs), which can isolate the CHX from the ambient and reduce the cooling power loss while also realizing acoustic field coupling between the adjacent cores.

The simulations of the proposed system are performed using SAGE software (Gedeon, 2013). SAGE can model and calculate the parameters of regenerative heat engines such as thermoacoustic machines and Stirling machines. To simulate the actual acoustic field, virtual pistons, i.e., a compression piston and an expansion piston, are used at the inlet and the outlet of the refrigerator. These pistons are massless models that are used to provide the inlet and outlet volume velocity amplitudes by adjusting their displacements and phase angles, which act as boundary conditions. The constraints and optimization goals are given during this optimization process. Meanwhile, to provide working space for massless pistons, the compression and expansion spaces are used which is slightly bigger than the half of the largest swept volume of these pistons.

In the model, several important variables, including the acoustic work, the coefficient of performance and the acoustic work utilization rate, are defined to describe the refrigerator's performance. The acoustic work is defined as

$$W_a = 1/2|p_1||U_1|\cos\theta_{pU} \tag{1}$$

where p_1 and U_1 are the pressure and volume velocity amplitudes, respectively. θ_{pU} represents the phase difference between the pressure and volume velocity waves.

The coefficient of performance (COP) is defined as

$$\mathrm{COP} = Q_c/(W_{in} - W_{out}) \tag{2}$$

where Q_c is the cooling power of the regenerator. W_{in} is the input acoustic work. W_{out} is the output acoustic work. W_{in}−W_{out} gives the acoustic work consumed. However, this COP actually represents the performance of the regenerator core and the output acoustic work which will be recovered in practice to reduce the input power, is not counted.

The input acoustic work utilization rate is defined as

$$\eta = (W_{in} - W_{out})/W_{in} \tag{3}$$

Basically, the acoustic work utilization rate should be increased as far as possible to produce higher cooling power with an acceptable COP.

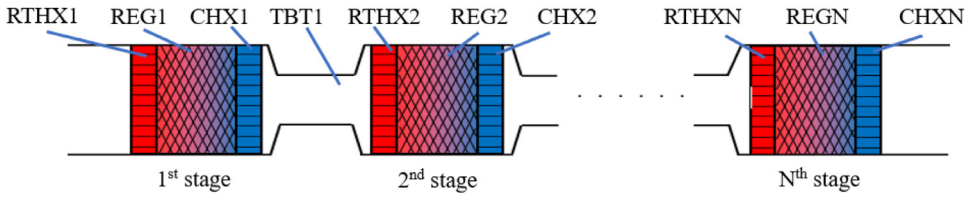

Fig. 1. Schematic of multi-stage TWTAR.

Table 1
Structural parameters of single-stage TWTAR.

components	inner diameter (mm)	Length (mm)	remarks
compression space			void volume of 2.6E-4 m^3
RTHX	130	40	shell-tube heat exchanger with porosity of 11.65%
REG	130	30	mesh screen with porosity of 76.9%, hydrodynamic radius of 42 μm
CHX	130	40	shell-tube heat exchanger with porosity of 12.39%
expansion space			void volume of 2.6E−4 m^3

3. Simulation results and discussion

First, the single-stage TWTAR is investigated to demonstrate the working characteristics of thermoacoustic refrigerators. Additionally, to determine whether a single-stage TWTAR can realize efficient input acoustic work utilization, the structural parameters of the regenerator and the virtual piston working conditions for the single-stage TWTAR are optimized to obtain the maximum cooling power. The influence of the number of stages on TWTAR performance is then investigated. Additionally, to gain a further understanding of the internal operating conditions of the multi-stage TWTAR, the cooling performance is presented for every stage. In the simulations, the working substance is helium, the mean pressure is 6 MPa, and the working frequency is 60 Hz. The ambient temperature is 313 K and the cooling temperature of the CHX is set at 273 K.

3.1. Single-stage TWTAR

From a thermoacoustic viewpoint, the regenerator is the only place in which the thermoacoustic effect occurs and the resulting acoustic work is used to pump the heat from the CHX to the RTHX; the cooling power can thus be obtained in the CHX. The structural parameters of the single-stage TWTAR used in the calculations are presented in Table 1. In particular, the TBT in the single-stage TWTAR is unnecessary because the temperature difference between the CHX and the ambient temperature is not large. The boundary conditions used in the simulations are as follows: the volume velocity of the compression piston is 9.44×10^{-3} m^3/s with a phase angle of 0°, the volume velocity of the expansion piston is 3.12×10^{-2} m^3/s with a phase angle of −55° and the input acoustic work is 3.0 kW.

Fig. 2 shows the axial distributions of the acoustic work and the total energy. The total energy is defined as the sum of the acoustic work and the exchanged heat. In the RTHX, the total energy decreased from 3.0 to 0.04 kW and approximately 2.96 kW of heat is thus rejected into the environment. In the regenerator, the acoustic work is consumed and is reduced from 2.90 to 2.32 kW. In addition, 2.17 kW of thermal energy is pumped from the CHX. The COP is approximately 2.73. However, the output acoustic work is 2.21 kW, which means that approximately 74% of the acoustic work is not used by the regenerator and the acoustic work utilization rate is thus only 0.26. This phenomenon is quite different under lower cooling temperature conditions; for example, the acoustic work utilization rate is approximately 0.8 when the cooling temperature is around 80 K (Hu et al., 2014).

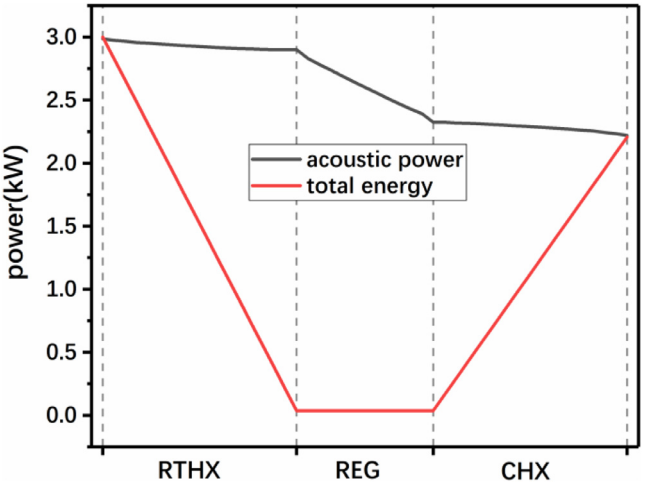

Fig. 2. Distributions of the acoustic work and the total energy of the single-stage TWTAR.

Fig. 3 shows the phase angle distributions of the pressure wave and the volume velocity oscillation and the difference between them. The phase angle of the pressure wave changes very little within the refrigerator. Because of the presence of the compression and expansion spaces at the two ends of the refrigerator, the phase angles of the volume velocity at the inlet and the outlet are changed to -27° and -52° respectively, which are different with those of pistons The phase angle differences between the pressure and volume velocity at inlet and outlet are 22° and 23°, respectively.

These numerical results appear to indicate that the single-stage TWTAR may inherently have a low utilization rate for the input acoustic work. To verify this viewpoint, performance optimizations at the maximum cooling power are performed with different regenerator diameters and lengths. During the optimization process, the input acoustic work remains fixed at 3 kW. Both the volume velocity and the phase angle of the virtual expansion piston are optimized to obtain the maximum cooling power. Fig. 4 shows the cooling power optimization results, including the acoustic work utilization rate, the cooling power and the COP, as functions of the length of the regenerator. As the length of the regenerator increases, more acoustic work can be consumed, and this is represented by an increase in the acoustic work utilization rate. However, the maximum cooling power and the COP decrease at the same time. Fig. 5 presents the cooling power optimization results

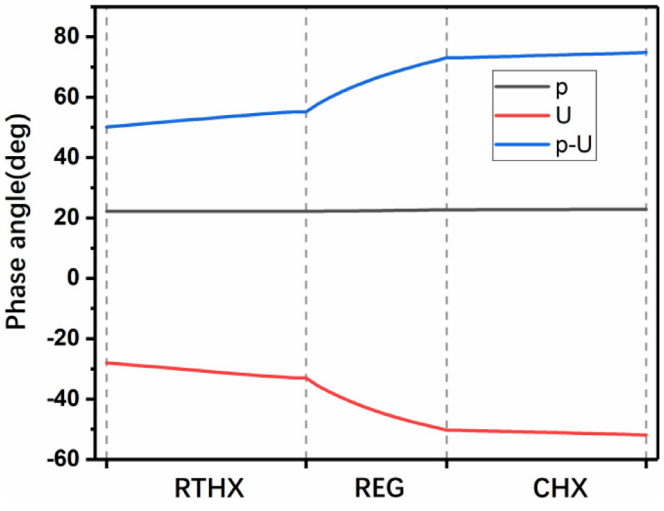

Fig. 3. Phase angle distributions of the pressure and the volume velocity and the difference between them for the single-stage TWTAR.

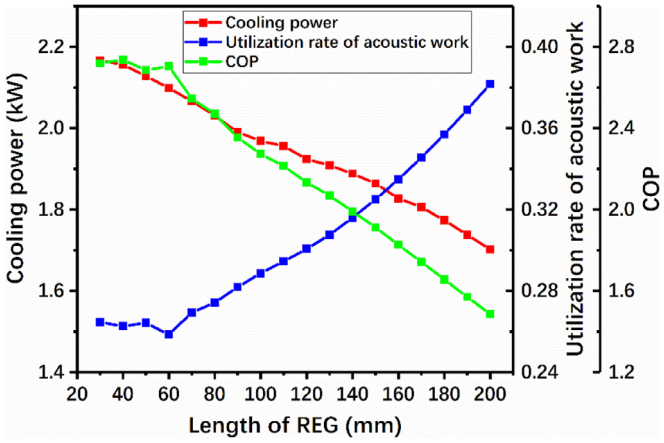

Fig. 4. Cooling power optimization results for different regenerator lengths.

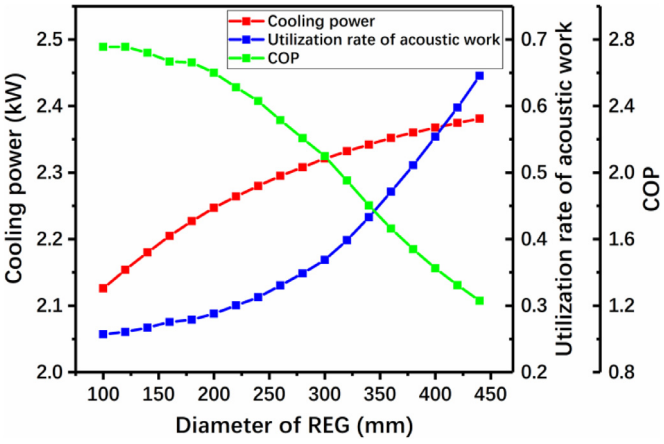

Fig. 5. Cooling power optimization results for different regenerator diameters.

for the different regenerator diameters. Both the maximum cooling power and the acoustic work utilization rate increase as the regenerator diameter increases. However, the acoustic work utilization value grows more rapidly than the cooling power, which results in a reduction in the COP.

Above-mentioned phenomena should be further analyzed for better comprehension. According to the thermoacoustic theory

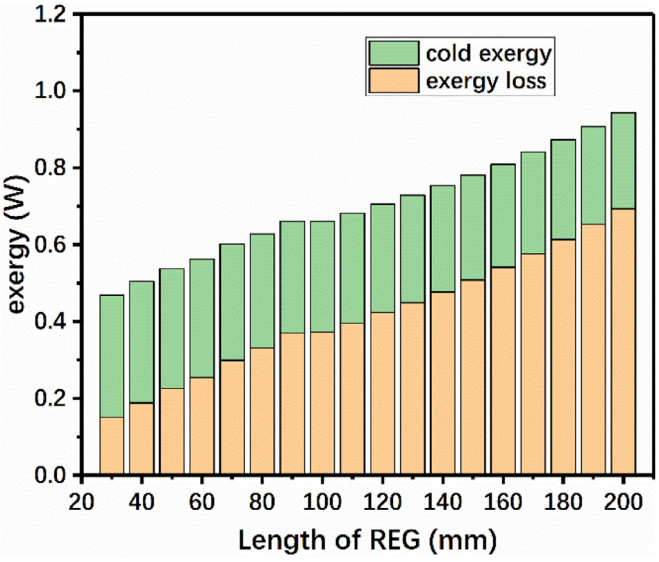

Fig. 6. Simulation results of cold exergy and exergy loss in REG with different regenerator lengths.

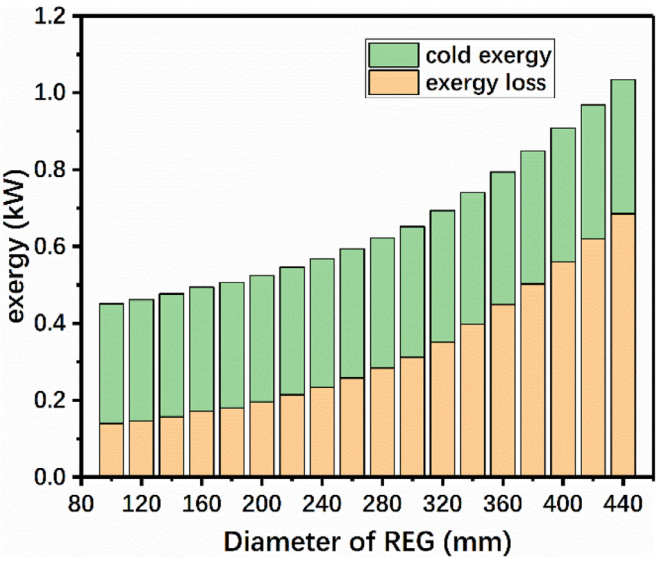

Fig. 7. Simulation results of cold exergy and exergy loss in REG with different regenerator diameters.

(Swift, 1999), the acoustic work is utilized by REG for: 1) heat pumping, i.e. the thermoacoustic effect; 2) irreversible loss, such as the viscous resistance loss, finite heat transfer loss between gas and solid wall, thermal conduction of the solid and gas; 3) other minor loss. The exergy analysis of the REG is performed to demonstrate the influences of the REG structural parameters on the acoustic work utilization. The utilized acoustic work is mainly converted to the cold exergy of the cooling power and the exergy loss. Fig. 6 and Fig. 7 show the simulation results of cold exergy and exergy loss as the functions of regenerator length and diameter. When the length of the REG increases, the exergy loss is greatly increase and cold exergy is slightly decrease. As a result, the acoustic work utilization is significantly improved while the COP is decreased. When the diameter of the REG increases, the exergy loss is also greatly increased while the cold exergy is slightly enhanced. As a result, the acoustic work utilization of REG is greatly increased while the COP is decreased. According to these optimization results, it indicates that although the acoustic

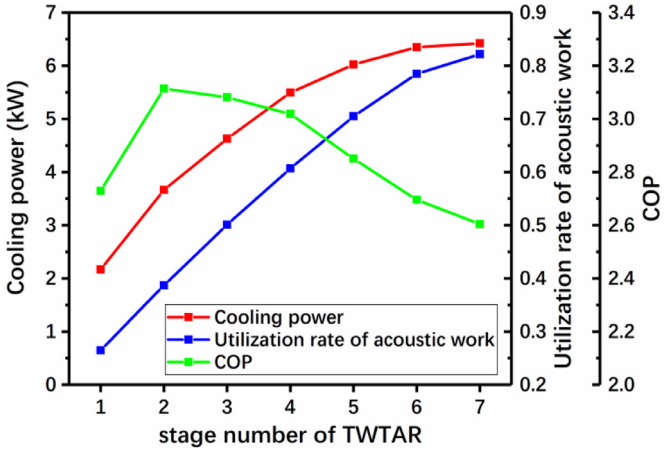

Fig. 8. Cooling power optimization results for the TWTAR with different numbers of stages.

work utilization can be greatly enhanced by changing the structural parameters of the regenerator, the cooling capacity cannot be changed. Thus, the COP is greatly decreased. New ways must therefore be found to solve this problem.

3.2. Multi-stage TWTAR

To solve the problem discussed above, the multi-stage TWTAR that is illustrated in Fig. 1 is proposed. In the next simulation, the structural parameters of the refrigerator core components, including the RTHX, the RGE and the CHX, are as same as those given in Table 1. To simplify the calculations and verify the idea easily, TBTs are used to connect the different refrigerator cores to isolate the CHX from the ambient temperature and to realize acoustic field coupling between the adjacent cores. During the simulations, the volume of every TBT and the volume velocity and phase angle of the expansion piston are optimized to achieve optimum performance in the multi-stage TWTAR. The operating parameters including the pressure, the frequency and the temperature remain unchanged and the boundary condition for the input acoustic work is still 3.0 kW.

Fig. 8 shows the calculation results for the optimum cooling powers of the different stages of the TWTAR. It can be seen from Fig. 8 that the maximum cooling power of the refrigerator increases along with the acoustic work utilization rate when the number of stages increases. The cooling power increases from 2.17 kW for a single-stage refrigerator to 6.42 kW for a seven-stage refrigerator, while the acoustic work utilization rate increases from 0.265 to 0.822. However, the speeds at which the cooling power and the acoustic work utilization rate increase become slower as the number of stages increases. The COP reaches an optimum value when the number of stages is two; more or fewer stages will result in a lower COP value. If the intention is to strike a balance between the cooling power and the COP, the four-stage TWTAR would be a good choice with its COP of 3.0, and would allow an acoustic work utilization rate of 0.6 and cooling power of 5.5 kW to be achieved. This represents a major improvement when compared with the single-stage system.

To enable further exploration of the operating mechanism of the multi-stage TWTAR, the distributions of the acoustic work, total energy and the phase angle difference between the pressure and the volume velocity within the refrigerators are presented in Fig. 9, which illustrates the changes in the acoustic work, total energy and the phase difference in detail. Fig. 9(a) shows that the acoustic work consumed by the regenerator decreases as the number of stages increases. It should be noted that even the number

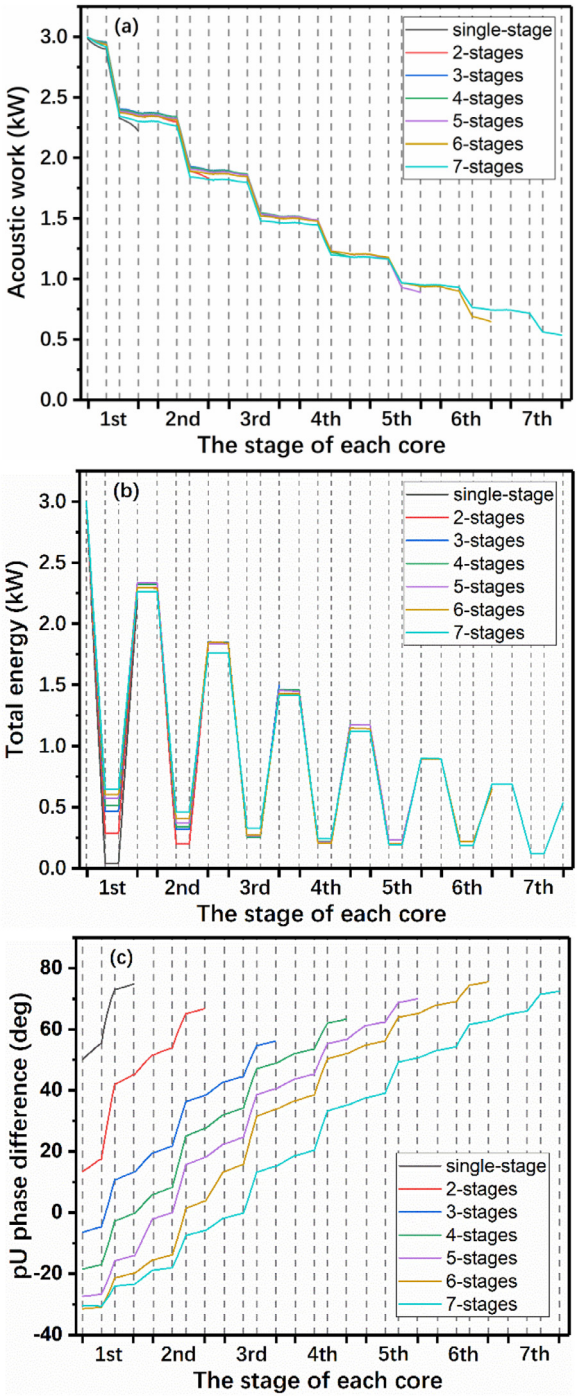

Fig. 9. Distributions of (a) acoustic work, (b) total energy and (c) phase difference in TWTAR.

of stages increases, the acoustic work consumed at the stage of the same order only changes slightly. Fig. 9(b) shows that the total energy of each core decreases as the number of stages increases. Meanwhile, the reduction of the total energy in the REG decreases at the stage of the same order. Fig. 9(c) shows that the phase angle difference at the inlet must generally decrease to achieve the highest cooling power as possible for the whole refrigerator. As the number of stages increases, the phase angle difference span between the inlet and the outlet is greatly increased.

Fig. 10 shows the optimum cooling power and the COP for every stage in the TWTAR. Fig. 10(a) shows that, in one refrigerator, the cooling power decreases stage by stage because of the reduc-

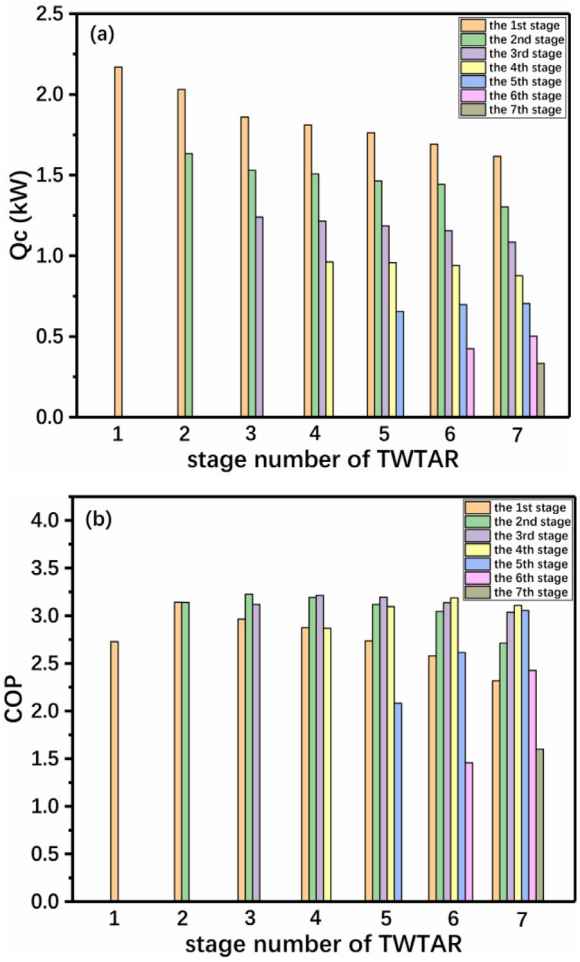

Fig. 10. Cooling power and COP for each refrigerator stage.

tion in the acoustic work that is input to each stage. As the number of stages increases, the cooling powers of the first to fourth stages decrease, while the cooling powers of the fifth and sixth stages increase slightly. Fig. 10(b) indicates that, in one refrigerator, the COP of each stage remains at a high level when the stage number is less than five. As the number of stages increases, the COP of each stage initially increases and then decreases. For larger numbers of stages, both the cooling power and the COP are greatly reduced. For example, in the seven-stage TWTAR, the cooling power of the seventh stage is only 0.3 kW and the COP is only approximately 1.7. This occurs because the phase angle difference between the pressure and the volume velocity is far from a suitable value and the number of stages should be an optimum value.

On the basis of the research described above, a three-stage TWTAR has been designed. All structural parameters with the exception of those of the first stage have been optimized. The SAGE software can perform the optimization automatically to find the best results; however, as more optimization variables are set, the optimization process becomes more difficult. Therefore, only a three-stage refrigerator has been optimized here. During the calculations, the inlet acoustic work of 3 kW and a COP of 3 are set as the constraints to meet the requirements of future applications. The optimization results for the structural parameters and performances are shown in Table 2. According to these results, total cooling power of 6.35 kW can be obtained with an acoustic work utilization rate of 0.71. In addition, the diameter of every stage should be greatly increased to achieve the optimum cooling performance. However, the acoustic work consumed, the cooling power and the

Table 2
Structural parameters and performances of the three-stage TWTAR.

	segment	inner diameter (mm)	Length (mm)	other parameters	cooling power (kW)	consumed acoustic work (kW)	COP
1st stage	RAHX1	130	40.0	tube diameter of 0.8 mm, porosity of 11.65%	2.067	0.664	3.113
	REG1		30.0	wire diameter of 50 μm, porosity of 76.90%, hydrodynamic radius of 42 μm			
	CHX1		40.0	tube diameter of 0.8 mm, porosity of 12.39%			
	TBT1			void volume of 616 cc			
2nd stage	RAHX2	233	22.6	tube diameter of 0.8 mm, porosity of 7.30%	1.729	0.512	3.377
	REG2		22.2	wire diameter of 50 μm, porosity of 80.67%, hydrodynamic radius of 52 μm			
	CHX2		16.2	tube diameter of 0.8 mm, porosity of 19.31%			
	TBT2			void volume of 2520 cc			
3rd stage	RAHX3	313	16.6	tube diameter of 0.8 mm, porosity of 19.74%	2.556	0.941	2.716
	REG3		32.2	wire diameter of 50 μm, porosity of 94.17%, hydrodynamic radius of 202 μm			
	CHX3		11.5	tube diameter of 0.8 mm, porosity of 43.76%			
total					6.352	2.117	3.0

COP of every stage all show different tendencies. An experiment setup will be designed in future work to verify the results of our simulation.

4. Conclusions

In this paper, the characteristics of traveling-wave thermoacoustic refrigerators operating at room temperature are investigated. First, the traditional single-stage traveling-wave thermoacoustic refrigerator is studied. The numerical results show that the low acoustic work utilization rate is difficult to enhance while maintaining good cooling performance. To solve these problems, the multi-stage traveling-wave thermoacoustic refrigerator is proposed and simulated. The calculation results show that the proposed multi-stage traveling-wave thermoacoustic refrigerator can effectively improve the acoustic work utilization rate. When compared with the single-stage refrigerator, the multi-stage refrigerator can increase the acoustic work utilization rate from 0.26 to more than 0.8 when only the size of the thermal buffer tube is optimized. Simultaneously, the maximum cooling power is also greatly improved while maintaining an acceptable cooling efficiency. As a result, the outlet acoustic work is greatly reduced and the work recovery process can be performed easily. However, as the number of stages increases, the cooling power and the cooling efficiency of the additional refrigerator cores decrease rapidly. Finally, a three-stage refrigerator has been designed by optimizing all structural parameters of the second and third stages. The results of simulations of this design will be used to build an experiment three-stage refrigerator setup in future work.

Declaration of Competing Interest

The authors declare that they have no known competing financial interests or personal relationships that could have appeared to influence the work reported in this paper.

Acknowledgements

Funding: This work was supported by the National Key Research and Development Program of China [grant number 2016YFB0901403]; and the Beijing Natural Science Foundation [grant number 3181002].

References

Ahmed, Hamza H.Ali, 2017. Performance-cost and global warming assessments of two residential scale solar cooling systems versus a conventional one in hot arid areas[J]. Sustain. Energy Technol. Assess. 20, 1–8.
Andrea, Brotzu, Felli, Ferdinando, Natali, Stefano, et al., 2015. Pipeline corrosion failure in an absorption chiller[J]. Sci. Direct 109, 43–54.
Athanasios, I.P, Alexio-Spyridon, K, et al., 2019. Absorption refrigeration process with organic working fluid mixtures-a review[J]. Renew. Sustain. Energy Rev. 109, 239–270.
Behzad, Monfared, Bjorn, Palm, 2018. Material requirements for magnetic refrigeration applications[J]. Int. J. Refrig. 96, 25–37.
Ceperley, P.H., 1979. A pistonless Stirling engine-the traveling wave heat engine[J]. J. Acoust. Soc. Am. 66 (5), 1508–1513.
Gedeon, D., 2013. Sage user's guide. Gedeon Associates, Athens.
Hu, J.Y., Luo, E.C., Dai, W., et al., 2007. A heat-driven thermoacoustic cryocooler capable of reaching below liquid hydrogen temperature. Chin. Sci. Bull. 52 (4), 574–576.
Hu, J.Y., Zhang, L.M., Zhu, J., et al., 2014. A high-efficiency coaxial pulse tube cryocooler with 500 W cooling capacity at 80 K[J]. Cryogenics 62, 7–10.
Jatinder, Gill, Jagdev, Singh, 2017. Energy analysis of vapor compression refrigeration system using mixture of R134a and LPG as refrigerant[J]. Int. J. Refrig. 84, 287–299.
Blok, Kees de, 2012. Multi-stage traveling wave thermoacoustics in practice. Presented at the 19th International Congress on Sound and Vibration.
Luo, E.C., Dai, W., Zhang, Y., et al., 2006. Thermoacoustically driven refrigerator with double thermoacoustic-Stirling cycles[J]. Appl. Phys. Lett. 88 (7), 074102.
Poese, Matthew E., 2004. An evolution of compact thermoacoustic refrigeration design[D]. the Pennsylvania State University, the United States.
Mckelvey, 1995. Shipboard electronics thermoacoustic cooler[J]. J. Acoust. Soc. Am. 98 (5), 2961.
Bassem, M.M., Ueda, Y., Akisawa, A., 2011. Design and construction of a traveling wave thermoacoustic refrigerator[J]. Int. J. Refrig. 34 (4), 1125–1131.
Radebaugh, R., McDermott, KM, Swift, GW, et al., 1990. Development of a thermoacoustically driven orifice pulse tube refrigerator. In: Proceedings of the interagency meeting on cryocoolers, Plymouth, MA, pp. 205–220.
Swift, G.W., Gardner, D.L., Backhaus, S., 1999. Acoustic recovery of lost power in pulse tube refrigerators[J]. J. Acoust. Soc. Am. 105 (2), 711–724.
Wang, H.Z., Zhang, L.M., Yu, G.Y., et al., 2019. A looped heat-driven thermoacoustic refrigeration system with direct-coupling configuration for room temperature cooling[J]. Sci. Bull. 64 (1), 8–10.
Xu, J.Y., Luo, E.C., Simone, H., 2020. Study on a heat-driven thermoacoustic refrigerator for low-grade heat recovery[J]. Appl. Energy 271.
Yu, B., Luo, E.C., Li, S.F., et al., 2011. Experimental study of a thermoacoustically–driven traveling wave thermoacoustic refrigerator[J]. Cryogenics 51, 49–54.